

## Coadsorbed NTCDI-melamine mixed phases on Ag-Si(111)

Luís M. A. Perdigão,<sup>1</sup> Giselle N. Fontes,<sup>1,2</sup> Ben L. Rogers,<sup>1</sup> Neil S. Oxtoby,<sup>3</sup> Gudrun Goretzki,<sup>3</sup> Neil R. Champness,<sup>3</sup> and Peter H. Beton<sup>1,\*</sup>

<sup>1</sup>*School of Physics and Astronomy, University of Nottingham, University Park, Nottingham NG7 2RD, United Kingdom*

<sup>2</sup>*Departamento de Física, ICEx, Universidade Federal de Minas Gerais, Avenida Antonio Carlos, 6627-Belo Horizonte, Minas Gerais CEP 30123-970, Brazil*

<sup>3</sup>*School of Chemistry, University of Nottingham, University Park, Nottingham NG7 2RD, United Kingdom*

(Received 25 April 2007; revised manuscript received 3 August 2007; published 5 December 2007)

The coadsorption of naphthalene tetracarboxylic diimide and melamine (1,3,5-triazine-2,4,6-triamine) on the Ag-Si(111) $\sqrt{3} \times \sqrt{3}R30^\circ$  surface has been investigated using scanning tunneling microscopy under ultrahigh vacuum conditions. Three hydrogen bonding arrangements between the constituent molecules are possible, which result in the formation of a variety of supramolecular structures. The primary unit for the formation of larger complex structures such as a triangular and a row arrangement was identified. A comparison with similar molecules which have been studied previously indicates that the molecule-substrate interaction plays an important role in the formation of the observed structures.

DOI: 10.1103/PhysRevB.76.245402

PACS number(s): 68.37.-d

## INTRODUCTION

The self-assembly of molecules in arrays stabilized by hydrogen bonding is a topic that is currently attracting great interest. Hydrogen bonding is rather weak compared with covalent bonding, but is a highly directional interaction and allows a degree of control in the formation of well ordered structures.<sup>1-9</sup> The growth of honeycomb arrangements using perylene tetracarboxylic diimide (PTCDI) and melamine mixtures has been demonstrated on Ag-Si(111) $\sqrt{3} \times \sqrt{3}R30^\circ$  and Au(111) surfaces,<sup>10,11</sup> where the triple-hydrogen bond between the PTCDI and melamine is known to stabilize the arrangement at room temperature. In previous work, it has also been shown that the same triple hydrogen bonding is responsible for the stabilization of other bimolecular networks on different surfaces.<sup>12-15</sup> Arrangements involving double-hydrogen bonds between constituent molecules are also possible such as in the structure of PTCDI and melamine islands.<sup>11,16</sup>

We have investigated the structures that the mixture of naphthalene tetracarboxylic diimide [NTCDI, Fig. 1(a)] and melamine [Fig. 1(b)] form on a Ag-Si(111) $\sqrt{3} \times \sqrt{3}R30^\circ$  surface. Previous studies on this surface demonstrated that many organic molecules diffuse at room temperature, allowing self-assembly to occur.<sup>9,10,12,16,17</sup> The NTCIDI molecule presents similarities with the PTCDI described above: it has the same diimide termination on both ends of the molecule, which may combine with melamine to form a triple-hydrogen bond [Fig. 1(c)]. The distance between the opposite nitrogen atoms in NTCIDI is approximately 7.0 Å, whereas in PTCDI, this value is 11.4 Å. This difference in molecular dimensions might be expected to lead to a direct analog of the hexagonal PTCDI-melamine network, but with a smaller period. However, the difference also leads to a removal of the commensurability between the surface lattice constant of the Ag-Si(111) $\sqrt{3} \times \sqrt{3}R30^\circ$  and the supramolecular network which is present for the PTCDI-melamine array. The study of the NTCIDI-melamine network is, therefore, expected to elucidate the importance of commensurability in stabilizing these structures. In fact, we found signifi-

cant differences for PTCDI-melamine mixed phases on the same surface. In particular, the combination of NTCIDI and melamine leads to a richer variety of structures. Although the order of these arrangements is short range, it is possible to identify more complex motifs which do display commensurability with the surface and form the basic building blocks of the structures observed.

## EXPERIMENTAL METHODS

The NTCIDI and melamine depositions were performed under ultrahigh vacuum conditions (base pressure  $<10^{-10}$  Torr). The Ag-Si(111) $\sqrt{3} \times \sqrt{3}R30^\circ$  surface was pre-

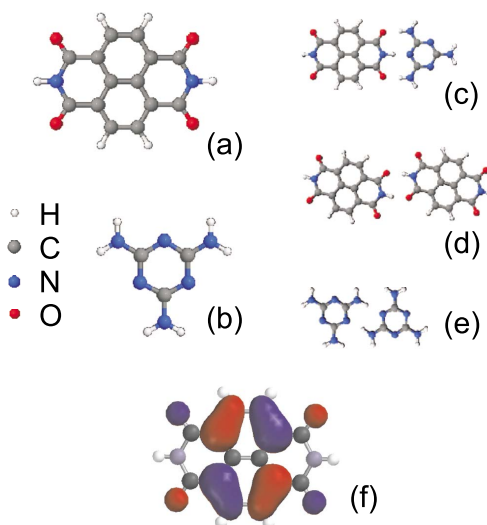


FIG. 1. (Color online) Molecular structures of (a) NTCIDI and (b) melamine. (c) Triple-hydrogen bond arrangement between NTCIDI and melamine. [(d) and (e)] Double-hydrogen bond arrangements of NTCIDI-NTCIDI and melamine-melamine, respectively. (f) Calculated HOMO orbital for NTCIDI (SPARTAN, density functional theory using B3LYP formalism and 6-311G\* basis set) with isosurfaces red and blue corresponding to positive and negative wave function amplitudes.

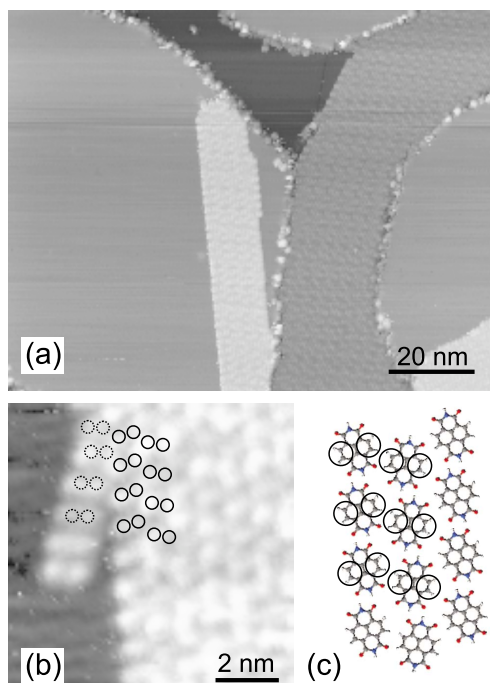


FIG. 2. (Color online) (a) STM images of two NTCDI islands on two distinct terraces of the Ag-Si(111) $\sqrt{3} \times \sqrt{3}R30^\circ$  surface, after deposition of 0.12 monolayer of NTCDI (sample bias of  $-2.5$  V and set point current of 50 pA). (b) Magnified view of the edge of a NTCDI domain. A short single row on the left leads to the identification of each NTCDI molecule to a double lobe in the image (two consecutive dashed circles). The double circles represent selected molecules. (c) Proposed molecular arrangement for the NTCDI domain in (b), with the circles representing the double lobes of the NTCDI molecules that were identified in (b) with unbroken circles.

pared by initially annealing the Si(111) substrate up to  $1200^\circ\text{C}$ , followed by sublimation of Ag with the sample held at  $500^\circ\text{C}$ . NTCDI and melamine were sequentially evaporated from separate cells at temperatures of  $180$  and  $90^\circ\text{C}$ , respectively. During NTCDI deposition, the sample was held at room temperature. Images of the surface were acquired using a scanning tunneling microscope (STM) operating in constant current mode at room temperature. NTCDI was synthesized using a procedure described elsewhere.<sup>17</sup>

## RESULTS AND DISCUSSION

Following submonolayer deposition of NTCDI onto the Ag-Si(111) $\sqrt{3} \times \sqrt{3}R30^\circ$  substrate, close-packed islands are observed in some images [Fig. 2(a)]. This observation is consistent with previous experiments reported in the literature.<sup>15,17</sup> NTCDI forms strongly faceted islands with an apparent height of  $\sim 1.7$  Å and with the molecules adopting a planar configuration on the surface. A high resolution image of the edge of a NTCDI domain is shown in Fig. 2(b), where each individual molecule can be identified as a double lobe. The highest occupied molecular orbital (HOMO) is

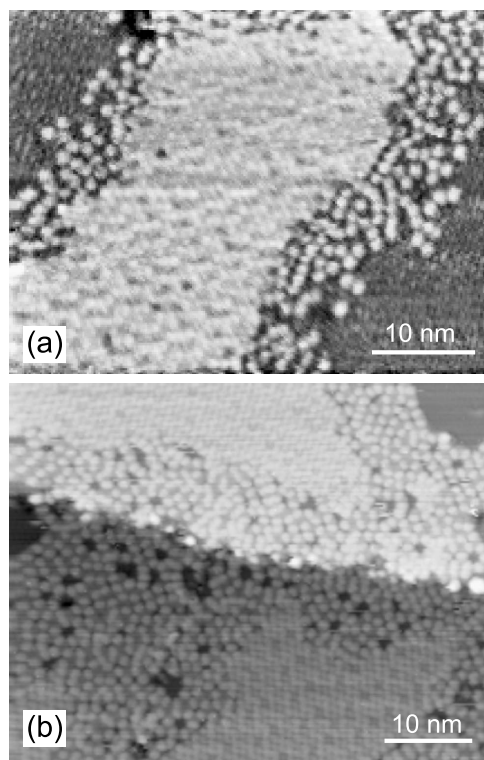


FIG. 3. (a) STM image of NTCDI after melamine deposition with sample at room temperature (operation parameters:  $-2.0$  V and 0.05 nA). (b) Image of NTCDI-melamine mixture following a gentle anneal at  $60$ – $80^\circ\text{C}$  for about 1 h.

shown in Fig. 1(f). Here, four maxima in probability density may be identified but, in common with our previous experimental work,<sup>17</sup> we observe two regions of high intramolecular contrast which we believe is due to resolution limitations of the instrument. The single row of NTCDI molecules on the left edge of the domain supports this identification. The circles drawn in the image illustrate an example of twelve NTCDI molecules that have been identified. The proposed molecular structure for the arrangement observed is shown in Fig. 2(c), consisting of rows of NTCDI molecules with alternating orientations from row to row, similar to the crystal structure of a single plane determined by x-ray diffraction.<sup>17</sup> Along the row, the measured periodicity for two molecules is  $\sim 20.1$  Å, which is consistent with twice the value of  $10.18$  Å determined in the diffraction measurements.<sup>17</sup> The apparent height of the molecules along the row alternates (every two molecules) with a faint variation of  $\sim 0.2$  Å, along which could be related to their placement relative to the reconstructed surface. For domains with other orientations, a different periodicity along the row is observed. The structure is stabilized by a double-hydrogen bond between adjacent molecules [Fig. 1(d)], leading to the formation of parallel rows. The interaction between neighboring rows in the bulk crystal involves a weak hydrogen bond between a C-H group and an oxygen atom from a molecule in an adjacent row.

The sample was subsequently exposed to melamine, with the sample held at room temperature. The resulting STM

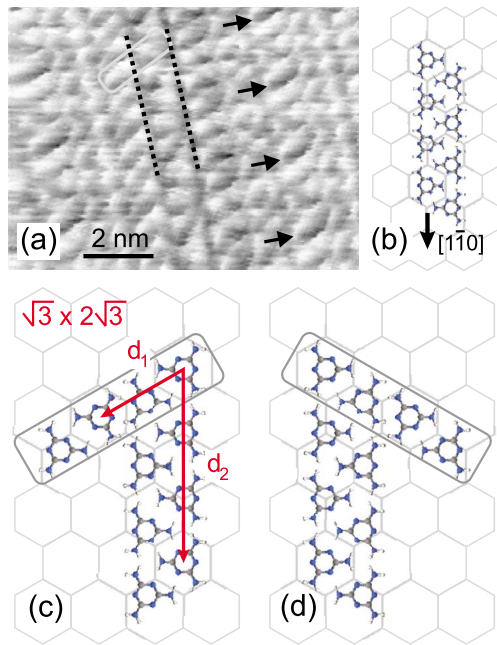


FIG. 4. (Color online) (a) High resolution image of a melamine domain (sample bias of  $-2$  V and set point current of  $50$  pA). Dashed lines represent the separation between double melamine rows. The gray rectangle indicates a tetramelamine chain across a double row and following direction  $d_1$  (see below). The arrows identify similar contrast features along one row. (b) Structure proposed for a single row which is parallel with one of the  $[1\bar{1}0]$  directions of the substrate. (c)  $\sqrt{3} \times 2\sqrt{3}$  arrangement proposed for the melamine domain, with unit cell vectors  $d_1$  and  $d_2$  defined locally. The gray rectangle shows a type of melamine stripe (see text). (d) Mirror reflection of structure (c). In the models, the hexagonal mesh represents the substrate reconstruction, with the centers of the hexagons corresponding to the silicon trimer positions according to the honeycomb-chain-trimer model of the Ag-Si(111) $\sqrt{3} \times \sqrt{3}R30^\circ$  surface (Ref. 19).

image in Fig. 3(a) shows that melamine has adsorbed in the surrounding areas of the NTCDI domains and that the borders of NTCDI have altered significantly. In a wide region around the pure NTCDI island, the melamine has led to a disruption of the domain, resulting in a mixed NTCDI-melamine phase. The molecular arrangement in this region appears rather disordered but, in some small locations, rows or trigonal shaped nodes can be identified. When a gentle annealing of  $60$ – $80$  °C is applied, most of the melamine desorbs, whereas the melamine participating in the mixed NTCDI-melamine phase remains on the surface [Fig. 3(b)]. The effect of the sample temperature (room temperature up to  $80$  °C) during the melamine deposition was found to have little importance on the resulting molecular arrangement. In an additional experiment, melamine was deposited onto the NTCDI/Ag-Si(111) $\sqrt{3} \times \sqrt{3}R30^\circ$  system with the substrate held at higher temperature, around  $60$ – $80$  °C. In STM images obtained on this sample, it was also found that NTCDI domains are surrounded by a mixed NTCDI-melamine region. The major difference we found with this preparation is that these mixed regions appeared wider compared to the

previous preparation, suggesting a greater degree of NTCDI-melamine mixing.

We were able to determine the structure of the melamine domains from images taken immediately after deposition, despite the difficulty related with the fact that melamine gradually desorbs from this surface at room temperature. The image in Fig. 4(a) shows a characteristic high resolution image of a melamine domain. We identify a characteristic row structure such as the one between the dashed lines. Consecutive rows have small differences in contrast, which we interpret to be a result of the different placement of the melamine molecules relative to substrate sites. The structure proposed for the row of molecules identified in Fig. 4(a) is shown in Fig. 4(b), where the molecules form a zigzag chain along the length of the row, with a double-hydrogen bond between each pair of molecules [Fig. 1(e)]. This double-hydrogen bond arrangement has been reported previously for melamine mixtures on Au(111),<sup>11</sup> leading to the formation of a hexagonal structure instead of the rows observed on this surface. Neighboring rows are connected also by a double-hydrogen bond between two melamine molecules. There are two configurations for this inter-row connection, and these are shown in Figs. 4(c) and 4(d). The relative placement of the melamine molecules between rows is slightly shifted upward or downward between each configuration. From the images, we estimate the distance between the rows to be approximately  $11.5 \pm 1$  Å, and the distance between two identically oriented melamine molecules along the row is about  $7.5 \pm 1$  Å. A distinct melamine chain following direction  $d_1$  is also highlighted with a gray rectangle. The importance of this will be clearer below when discussing the NTCDI-melamine arrangements. It is possible that this linear arrangement may form a regular arrangement relative to the surface. This chain makes an angle of approximately  $60^\circ$  with the zigzag row direction (direction  $d_2$ ).

Although the substrate reconstruction is not visible in the images, we were able to estimate the relative orientation of the melamine domain with the reconstructed Ag-Si(111) $\sqrt{3} \times \sqrt{3}R30^\circ$  surface by collecting images of the substrate prior to the deposition. We found that both the zigzag row and the linear tape follow closely one of the surface  $[1\bar{1}0]$  directions. Moreover, there is a regular variation of contrast along the row direction as indicated with arrows in Fig. 4(a) pointing at identical features, each corresponding to a melamine molecule. As there are two melamine molecules between the indicated ones and with the same orientation, this suggests that every three melamine molecules along the row are sitting at equivalent surface sites.

Based on these observations, we propose the commensurate arrangement shown in Fig. 4(c) that has  $\sqrt{3} \times 2\sqrt{3}$  periodicity (vectors  $d_1$  and  $d_2$ ) relative to the Ag-Si(111) $\sqrt{3} \times \sqrt{3}R30^\circ$  reconstructed surface. This may apply to two or more consecutive rows depending on the way they are interconnected. The vertices of the regular triangular mesh arrangement in Fig. 4(b) represent the silicon trimer positions of the reconstructed Ag-Si(111) $\sqrt{3} \times \sqrt{3}R30^\circ$  surface,<sup>18</sup> and the position of the melamine molecules relative to the surface sites is approximate. Note that our model addresses only the separation of molecules, not their absolute registry with



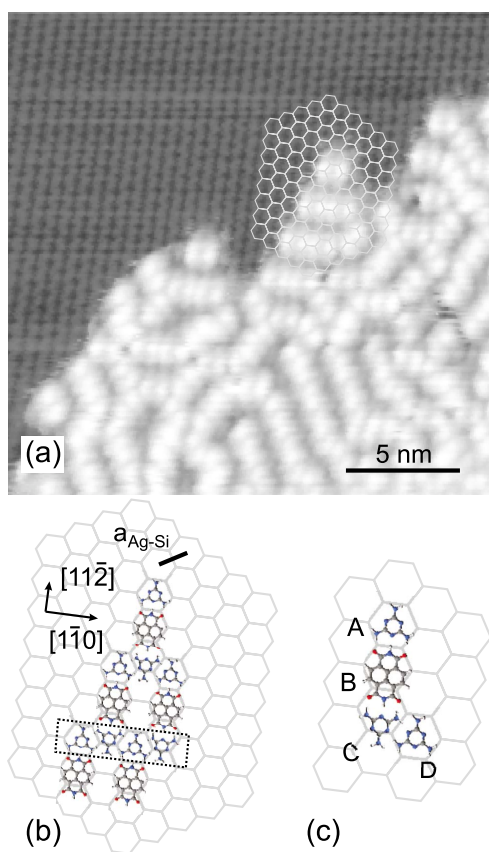


FIG. 5. (Color online) (a) Image of NTCDI-melamine mixed region (sample bias of  $-2.3$  V, set point current of  $50$  pA, and dimensions given in scale bar). Superimposed is the hexagonal mesh that represents the reconstructed surface, where the centers correspond to silicon trimer sites that appear with darker contrast in images. A model for the molecular arrangement covered by the hexagonal mesh is represented in (b). The position of the NTCDI molecules was determined from the double lobes in the STM image, and the melamine was inferred based on the triple-hydrogen bond arrangement that melamine and NTCDI form. A row of melamine molecules stabilized by double-hydrogen bonds is highlighted with a dashed rectangle. The simplified NTCDI-melamine arrangement shown in (c) verifies the commensurability with the reconstructed  $\text{Ag-Si}(111)\sqrt{3}\times\sqrt{3}R30^\circ$  surface, whereby both melamine molecules labeled as A and D are located above a silicon trimer position.

the surface. According to this model, the values for the unit cell vectors are  $d_1=11.5$  Å and  $d_2=23.0$  Å, corresponding to a spacing between two adjacent molecules along the row  $d_2/3=7.7$  Å, in agreement with the measured value given above.

We note that the arrangement observed for the melamine domains on this surface is significantly different compared with the hexagonal structure it forms on the  $\text{Au}(111)$  surface.<sup>11,13</sup> On both substrates, pairs of melamine molecules form double-hydrogen bonds.

We now consider the NTCDI-melamine mixed phase. Figure 5(a) shows a higher resolution image obtained on one of these regions, where the substrate reconstruction is also clear. The position and direction of individual NTCDI mol-

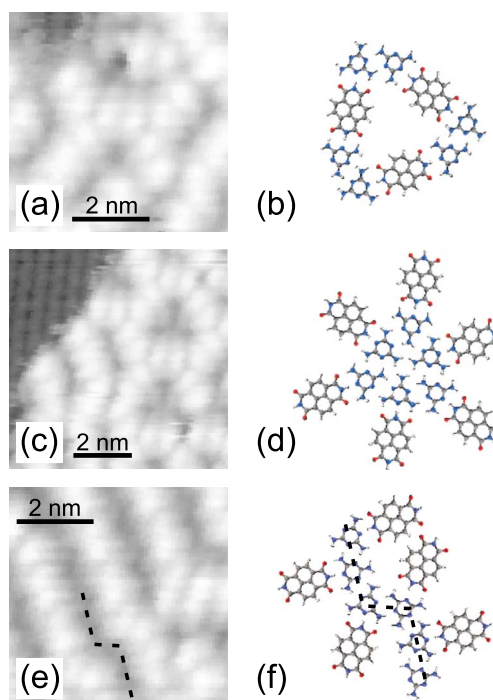


FIG. 6. (Color online) Some identified NTCDI-melamine structures (left) and corresponding molecular arrangement (right): triangular [(a) and (b)], star [(c) and (d)], and melamine tape [(e) and (f)] highlighted with a dashed line. Dimensions of each image are given in the scale bar. Operation parameters for all STM images were  $-2.3$  V sample bias and set point current of  $50$  pA.

ecules are relatively easy to deduce. Each double-lobe feature is assigned to one NTCDI molecule and its orientation determined, as explained above [Fig. 1(f)]. Melamine molecules are difficult to resolve due to their low contrast, but their placement could be inferred from the position and orientation from neighboring NTCDI molecules. By extending the hexagonal mesh over the parallel row arrangement, the registry of the NTCDI and melamine molecules relative to the surface reconstruction could be determined, resulting in the structure shown in Fig. 5(b). In this structure, melamine is bonded with the NTCDI molecules by a triple-hydrogen bond, and a double-hydrogen bond between two melamine molecules [Fig. 1(e)] stabilizes the arrangement. In the row arrangement, NTCDI molecules are clearly aligned parallel to one of the  $[11\bar{2}]$  directions of the  $\text{Ag-Si}(111)\sqrt{3}\times\sqrt{3}R30^\circ$  substrate, and in between the rows, a chain of melamine molecules follows the  $[1\bar{1}0]$  direction. The positions of the NTCDI centers appear less than  $1$  Å away from a silicon trimer position. The centers of the melamine molecules are located on two possible positions, one of which is less than  $0.5$  Å from the silicon trimer locations. From this observation, it is straightforward to establish the simplified arrangement shown in Fig. 5(c). For the following discussion, each molecule was labeled with A, B, C, and D as shown. According to this model, both melamine A and D sit at equivalent positions, over a silicon trimer, whereas melamine C, which corresponds to the sites of half the melamine molecules, sits at a distinct position. Moreover, the

distance between melamine A and D can be determined from the model to be  $d_{A-D} = (\sqrt{29}/2)a_{\text{Ag-Si}} \sim 17.5 \text{ \AA}$ , with  $a_{\text{Ag-Si}} = 6.65 \text{ \AA}$  being the periodicity of the reconstructed surface. This value differs only slightly from the estimated value determined for the optimized geometry of the same arrangement, which was found to be  $d_{A-D} = 17.85 \text{ \AA}$ , and the same calculation also gave  $d_{A-C} = 15.48 \text{ \AA}$ .<sup>19</sup>

The formation of the melamine stripe highlighted in Fig. 5(b) with a dashed rectangle also appears as a structural unit in the assembly of the pure melamine phase [see Fig. 4(c)].

In addition to the row structure, other arrangements can be identified within the NTCDI-melamine mixed region. Figures 6(a), 6(c), and 6(e) are some examples of these, and, based on the position and orientation of the NTCDI species inferred from their double-lobe appearance, the proposed arrangements are shown in Figs. 6(b), 6(d), and 6(f), respectively. The trigonal structure in Fig. 6(a) is often observed, and its triangular structure shown in Fig. 6(b) indicates that this is composed of three units identical to the structure shown in Fig. 5(c). The star-shaped structure in Fig. 6(d) is the proposed arrangement for the center of each triangle that appears in Fig. 6(c). Six melamine molecules form a hydrogen bonded arrangement which has some similarities with the melamine ordered phase.

Finally, the twisted appearance of the molecular structure in Fig. 6(e) is attributed to the formation of a linked melamine chain such as shown in Fig. 6(f). This arrangement can be seen as a possible extension of the melamine chain previously highlighted with a dashed rectangle in Figs. 5(b) and 4(c), while also maintaining the requirement of commensurability with the substrate.

We stress that the much greater variety of arrangements observed for the NTCDI-melamine system is a direct consequence of the formation of melamine-melamine bonding, which is not seen for the PTCDI-melamine on this surface<sup>10</sup> but has been reported on Au(111).<sup>11</sup> The observed structures for this system are in strong contrast with the honeycomb arrangements observed with PTCDI-melamine mixtures on the same surface,<sup>10</sup> where it was found that all melamine species in the hexagonal network sit perfectly on top of silicon trimers. If these PTCDI molecules were replaced by NTCDI species, the resulting honeycomb structure would not be commensurate. This is clearly demonstrated in Fig. 5(c) by comparing the position of melamine molecules A and C relative to the substrate. The addition of melamine D fulfills the requirement of commensurability of the structure, but it also constrains melamine C from forming a triple-hydrogen bond with a neighboring NTCDI along this direction.

The calculated stabilization energies of NTCDI-melamine and melamine-melamine junctions in gas phase are respectively  $-0.84$  and  $-0.55 \text{ eV}$ ,<sup>19</sup> hence the NTCDI-melamine junction is more favorable. However, our results seem to suggest that there is no prevalence in the formation of NTCDI-melamine junctions since melamine-melamine and NTCDI-NTCDI arrangements appear abundant in the images. The observation of commensurate subunits of these structures provides strong evidence that the molecule-substrate interaction also plays a significant role in the stabilization of the observed arrangements. For a commensurate

arrangement, all the molecules may adopt favorable adsorption sites on the surface. The arrangements determined from the images and our previous work suggest that one energetically favorable site for the melamine is on top of silicon trimer sites.

According to the models proposed for the row or triangular arrangements, it should be possible to have large areas of the surface covered with a single ordered domain. However, no large domains of the same regular arrangement were observed. The reason for this could be attributed to either the shape of the primary unit and the geometric linkage sites between the units [Fig. 5(c)] or a substrate mediated effect. Starting from melamine labeled as A in Fig. 5(c), there are three possible ways that NTCDI may link with this melamine, and then six possible sites where the next melamine may be found on an equivalent site, above the silicon trimer position. Additional linkage with NTCDI and melamine species leads to a large number of possible arrangements. This number could be lowered if additional constraints or forces were present that could reduce the likelihood of certain arrangements and eventually lead to more regular structures. From the energetic point of view, we would expect larger domains corresponding to the structure which is most energetically favorable. Although it is possible to perform a calculation that would allow us to establish the lowest energy structure from those proposed, such a numeric calculation would be complex as it would need to involve the surface interaction. Nevertheless, the difference in energy between different arrangements built from the same primary unit would be very low compared to the strength of the hydrogen bonds. This is due to a relatively large distance between the component molecules in different units. Although substrate mediated interaction has been proposed as a mechanism for large range intermolecular interaction and self-assembly observed in certain systems,<sup>20,21</sup> this seems unlikely to apply to the NTCDI-melamine on the Ag-Si(111) $\sqrt{3} \times \sqrt{3}R30^\circ$  system.

## CONCLUSION

It was demonstrated that the NTCDI and melamine mixtures on a Ag-Si(111) $\sqrt{3} \times \sqrt{3}R30^\circ$  surface can be decomposed into identical primary units which are commensurate with the surface. Three secondary arrangements were also identified and discussed. It is proposed that the absence of constraints on the molecular interactions and the geometry of the primary unit may justify the lack of long range ordered structures observed. These results provide an insight into the importance of the balance between intermolecular interactions and commensurability in the formation of ordered self-assembled structures on surfaces.

## ACKNOWLEDGMENTS

This work was supported by the U.K. Engineering and Physical Sciences Research Council (EPSRC) under Grant No. GR/S97521/01. G.N.F. is grateful for the financial support from CAPES (Brazil).

\*Corresponding author. FAX: +44 115 951 5180; peter.beton@nottingham.ac.uk

- <sup>1</sup>J. V. Barth, J. Weckesser, C. Cai, P. Günter, L. Bürgi, O. Jeandupeaux, and K. Kern, *Angew. Chem., Int. Ed.* **39**, 1230 (2000).
- <sup>2</sup>S. Griessl, M. Lackinger, M. Edelwirth, M. Hietschold, and W. M. Hechl, *Single Mol.* **3**, 25 (2002).
- <sup>3</sup>A. Dimitriev, N. Lin, J. Weckesser, J. V. Barth, and K. Kern, *J. Phys. Chem. B* **106**, 6907 (2002).
- <sup>4</sup>M. Stöhr, M. Wahl, C. H. Galka, T. Riehm, T. A. Jung, and L. H. Gade, *Angew. Chem., Int. Ed.* **44**, 7394 (2005).
- <sup>5</sup>R. Otero, M. Schöck, L. M. Molina, E. Lægsgaard, I. Stensgaard, B. Hammer, and F. Besenbacher, *Angew. Chem.* **117**, 2 (2005).
- <sup>6</sup>S. Xu, M. Dong, E. Rauls, R. Otero, T. R. Linderoth, and F. Besenbacher, *Nano Lett.* **6**, 1434 (2006).
- <sup>7</sup>S. De Feyter and F. C. De Schryver, *Chem. Soc. Rev.* **32**, 139 (2003).
- <sup>8</sup>T. Yokoyama, S. Yokoyama, T. Kamikado, Y. Okuno, and S. Mashiko, *Nature (London)* **413**, 619 (2001).
- <sup>9</sup>L. M. A. Perdigão, P. A. Staniec, N. R. Champness, R. E. A. Kelly, L. N. Kantorovich, and P. H. Beton, *Phys. Rev. B* **73**, 195423 (2006).
- <sup>10</sup>J. A. Theobald, N. S. Oxtoby, M. A. Phillips, N. R. Champness, and P. H. Beton, *Nature (London)* **424**, 1029 (2003).
- <sup>11</sup>L. M. A. Perdigão, E. W. Perkins, J. Ma, P. A. Staniec, B. L. Rogers, N. R. Champness, and P. H. Beton, *J. Phys. Chem. B* **110**, 12539 (2006).
- <sup>12</sup>L. M. A. Perdigão, N. R. Champness, and P. H. Beton, *Chem. Commun. (Cambridge)* 2006, 538.
- <sup>13</sup>P. A. Staniec, L. M. A. Perdigão, B. L. Rogers, N. R. Champness, and P. H. Beton, *J. Phys. Chem. C* **111**, 886 (2007).
- <sup>14</sup>M. E. Cañas-Ventura, W. Xiao, D. Wasserfallen, K. Müllen, H. Brune, J. V. Barth, and R. Fasel, *Angew. Chem., Int. Ed.* **46**, 1814 (2007).
- <sup>15</sup>M. Ruiz-Osés, N. González-Lakunza, I. Silanes, A. Gourdon, A. Arnau, and J. E. Ortega, *J. Phys. Chem. B* **110**, 25573 (2006).
- <sup>16</sup>J. C. Swarbrick, J. Ma, J. A. Theobald, N. S. Oxtoby, J. N. O'Shea, N. R. Champness, and P. H. Beton, *J. Phys. Chem. B* **109**, 12167 (2005).
- <sup>17</sup>D. L. Keeling, N. S. Oxtoby, C. Wilson, M. J. Humphry, N. R. Champness, and P. H. Beton, *Nano Lett.* **3**, 9 (2003).
- <sup>18</sup>K. J. Wan, X. F. Lin, and J. Nogami, *Phys. Rev. B* **47**, 13700 (1993).
- <sup>19</sup>Geometry optimization calculations using Materials Studio DMOL3 density function theory package. Atom positions were constrained to the same plane. The exchange-correlation potential used was the generalized gradient approximation with Perdew-Burke-Ernzerhof gradient correction. Double numerical plus polarization basis set was used with no core treatment and with orbital cutoff set to medium.
- <sup>20</sup>G. Pawin, K. L. Wong, K.-Y. Kwon, and L. Bartels, *Science* **313**, 961 (2006).
- <sup>21</sup>P. Hyldgaard and M. Persson, *J. Phys.: Condens. Matter* **12**, L13 (2000).